Optimisation of vortex tube thermal performance by CFD simulation

Quentin Sorel, Bénédicte Champel, Quynh Trang Pham

OPTIMISATION OF VORTEX TUBE THERMAL PERFORMANCE BY CFD SIMULATION

Quentin Sorel[1], Bénédicte Champel[1], Quynh Trang Pham[1*]

[1]CEA Grenoble, 17 Avenue des Martyrs, 38000 Grenoble, France

ABSTRACT

A vortex tube is a thermal device that splits a pressurized gas stream towards two lower pressure exits: cold gas on one side and hot gas on the other. Due to its small size and simple design with no moving parts, it is widely used for varying industrial cooling applications. The tangential injection of compressed gas into the tube generates a swirl flow movement. However, the physical phenomenon producing the temperature separation in the tube is still not fully understood. The current research work presents a CFD study of vortex tubes with Ansys Fluent™. 3D simulation of a selected tube vortex design has been realized in order to identify and investigate the influence of input parameters on the thermal performances of vortex tubes. A geometric optimization is conducted in order to improve the performance of such device. An analysis of the simulation results raises the question of Mach number and supersonic outlet velocities, which would be of interest for further study on vortex tube.

KEY WORDS: CFD, vortex tube, optimization, supersonic flow

1. INTRODUCTION

Vortex tube is a device that splits an incoming high pressure gas stream into two streams of lower pressure: one outgoing stream has a higher temperature and the other one has a lower temperature than the inlet gas. This phenomenon is known as temperature separation or energy separation effect. The vortex tube was first invented by French physicist Ranque [1].
A vortex tube is composed of a tube, a set of tangential nozzles at inlet, a conical valve at hot stream outlet, and an orifice at cold stream outlet. According to the relative location of the cold and hot outlets, two types of vortex tubes can be identified: (i) parallel flow vortex tubes, where the two outlets are located on the same side of the tube and (ii) counter flow vortex tube, where cold and hot outlets are located in the opposite direction to each other. The latter type avoids mixing of hot and cold mass of working gas, thus performing superior to parallel flow vortex tube.
Vortex tubes have several advantages over the conventional refrigerating devices: absence of moving parts, simple and compact design, no refrigerant used, low maintenance, long operational life… Traditionally they have been used extensively for cooling machine parts or electronic cabinets, or dehumidifying gas samples. Another application of vortex tubes, first proposed by Linderstrom-Lang in 1964 [2], consists in separating gas species from a mixture.

First experiments to study the effect of tube geometry were carried out by Hilsch [3] in 1947. In the 60-70s, Takahama also reported various relationships between the different parameters of the vortex tube ([4], [5]). Later, many experimental and numerical studies have been carried out in order to guide the design of new tubes (see [6], [7], [8], [9] or [10] for reviews).
Operating conditions (inlet and outlet pressures, working fluid…) also exert an impact on vortex tubes' performance. It has been shown that tube performance is better if pressure loss ratio increases ([11], [12]). Another important factor affecting the separation effect is the cold mass fraction ε that is defined

as the ratio of cold mass flow over inlet mass flow. Two general trends can be found in the literature regarding the impact of cold mass fraction on cold temperature gradient:

- Some papers state that the maximum cooling effect occurs when the cold mass fraction reaches a value around 30% (see for example the experiments by [13], [14] or [15], and CFD results by [16] and [17]).
- Others present a linear evolution of cold temperature gradient with cold mass fraction ([11], [18]).

The purpose of this article is to present a numerical study aiming at finding the optimal design of a vortex tube in order to maximize cold temperature gradient. Cold temperature gradient (ΔTc) is one of the performance indicators of vortex tubes. It is calculated as the difference between inlet air temperature T_i and cold side air temperature T_c :

$$\Delta T_c = T_i - T_c \tag{1}$$

In the frame of this study, unexpected behaviours were predicted numerically regarding the evolution of cold temperature gradient with inlet pressure, and with cold mass fraction. To the authors' knowledge, these behaviours that were obtained for specific conditions, were not described previously in the literature. The behaviour seems to be linked to the evolution of Mach number on cold outlet. However, a proper understanding of the effect is still missing.

The article is separated into three sections. Section 2 presents the initial tube geometry and the numerical model developed. Section 3 presents the choice of the turbulence model and the comparison of model to experimental results. Section 4 presents prospective results from the model, mainly the impact of inlet pressure on cold temperature gradient, and the evolution of cold temperature gradient with cold mass fraction for initial and optimized tubes. The evolution of Mach number at cold outlet, and its distribution, are also presented, that suggest possible links with the phenomena observed.

2. NUMERICAL MODEL

2.1 Geometry

The geometry considered for the model corresponds to the configuration that was characterized experimentally by Dincer et al. [19]. Numerical models of this configuration were carried out later on by Baghdad et al [20] and Ouadha et al [21].

The total length of the tube is 145mm: 133mm for the hot part, 10mm for the cold exit, and 2mm for the vortex chamber (Figure 1).

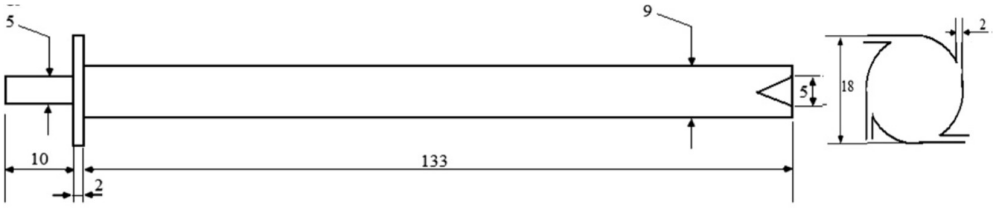

Fig. 1 Geometry of the vortex tube considered (after [20])

Given the four entry nozzles, a periodical model representing one fourth of the total volume is considered.

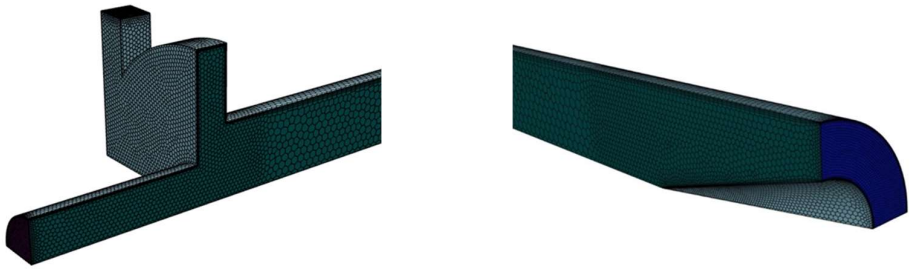

Fig. 2 Geometry of the model (inlet and cold outlet to the left, hot outlet to the right)

2.2 Boundary conditions

The following boundary conditions are defined (Figure 3):

- At the inlet, total pressure and total temperature are fixed.
- At the cold outlet, total pressure is fixed (at the atmospheric pressure).
- At the hot outlet, total pressure is fixed at a value slightly over atmospheric pressure. This overpressure is the parameter through which the cold mass fraction is controlled. Indeed, when this overpressure increases, cold mass fraction increases. This method of controlling cold mass fraction has been widely used in literature ([11], [18], [22]).
- The walls are considered adiabatic.
- Finally, two surfaces have a periodicity condition in rotation (the air flow leaving one surface corresponds to the air flow entering the other surface).

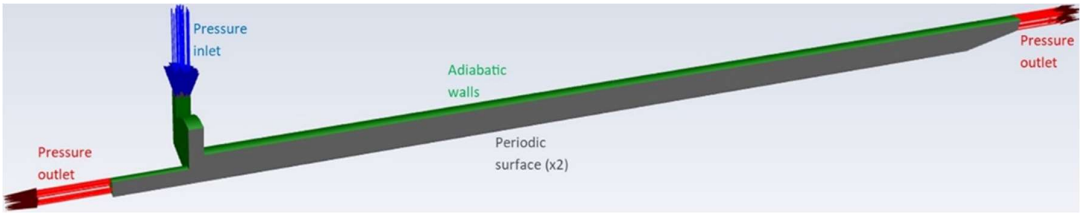

Fig. 3 Boundary conditions

2.3 Governing equations

The simulation of the stream field in the vortex tube is carried out in steady-state using Ansys Fluent™ 2022.R1. The fluid is considered to be dry air. The flow is considered to be 3-D compressible and turbulent. Gravity is not considered.

The governing equations solved by Fluent™ are the Continuity equation (2), Momentum equation (3) and Energy equation (4), as follows:

$$\frac{\partial \rho u_i}{\partial x_i} = 0 \tag{2}$$

$$\frac{\partial}{\partial x_j}\left(\rho u_i u_j\right) = -\frac{\partial p}{\partial x_i} + \frac{\partial \tau_{ij}}{\partial x_j} + \frac{\partial}{\partial x_j}\left(-\rho\overline{u_i' u_j'}\right) \tag{3}$$

$$\frac{\partial}{\partial x_i}\left(u_i(\rho E + p)\right) = \frac{\partial u_i \tau_{ij}}{\partial x_j} + \frac{\partial q_j}{\partial x_j} \tag{4}$$

Where ρ, u_i, p and E denote density, velocity components in x, y and z directions, the static pressure, and the volumetric total energy.

Viscosity is taken into account in the deviatoric stress tensor:

$$\tau_{ij} = \mu\left(\frac{\partial u_i}{\partial x_j} + \frac{\partial u_j}{\partial x_i}\right) - \frac{2}{3}\mu\frac{\partial u_i}{\partial x_i}\delta_{ij} \quad (5)$$

The total energy is given by:

$$E = c_v T + \frac{u_i^2}{2} - \frac{p}{\rho} \quad (6)$$

and the effective thermal conductivity is given by:

$$k_{eff} = k + \frac{c_p \mu_t}{Pr_t} \quad (7)$$

The equation of state is required to relate pressure, volume and temperature in compressible flows. We consider here dry air as a perfect gas:

$$\rho = \frac{p}{rT} \quad (8)$$

The pressure based, implicit-coupled solver is used. This solver is advised for studies where Mach number is under 2 (which is the case in our study).

2.4 Meshing

A poly-hexcore type mesh is used.

A sensitivity study has been performed on the mesh quality in order to set the cells' number. The final mesh includes 300 000 cells, which corresponds to a maximum cell size of 2mm. The analysis of the final mesh shows that 90% of cells have a skewness under 0.1, and 90% of cells have an orthogonal quality over 0.9, which is satisfactory.

3. MODEL VALIDATION

In a first step, a sensitivity analysis on the turbulence model has been performed. Standard k-ε, Realizable k- ε and RSM models have been compared with each other and with the experimental data from Dincer et al [19] with an inlet pressure of 380kPa.

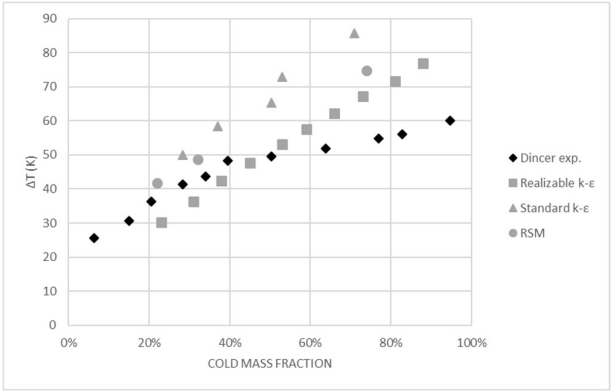

Fig. 4 Performance of turbulence models in predicting experimental measurements (inlet pressure 380kPa)

As can be seen in Figure 4, the evolution of total temperature gradient with cold mass fraction observed experimentally is linear in two parts, with a lower slope at cold mass fractions above 40%. None of the models correctly reproduces this decrease in slope at high cold mass fractions.

The Realizable k- ε model is the one that gives the results closer to the experimental data. In particular this model gives better results than the RSM turbulence model, that was selected by Baghdad et al [20] and Ouadha et al [21] based on the same experimental study by Dincer at al [19]. However, those authors did not test the Realizable k-ε model.

In a second step, the predictions from our model, using the Realizable k- ε model, are compared with Dincer et al. [19] experimental measurements for the four inlet pressures ranging from 200kPa to 380kPa. As can be seen in Figure 5, the predictions from our model are closer to the experiments for low inlet pressures than for high inlet pressures (this was already the case in the study by Baghdad et al [20]).

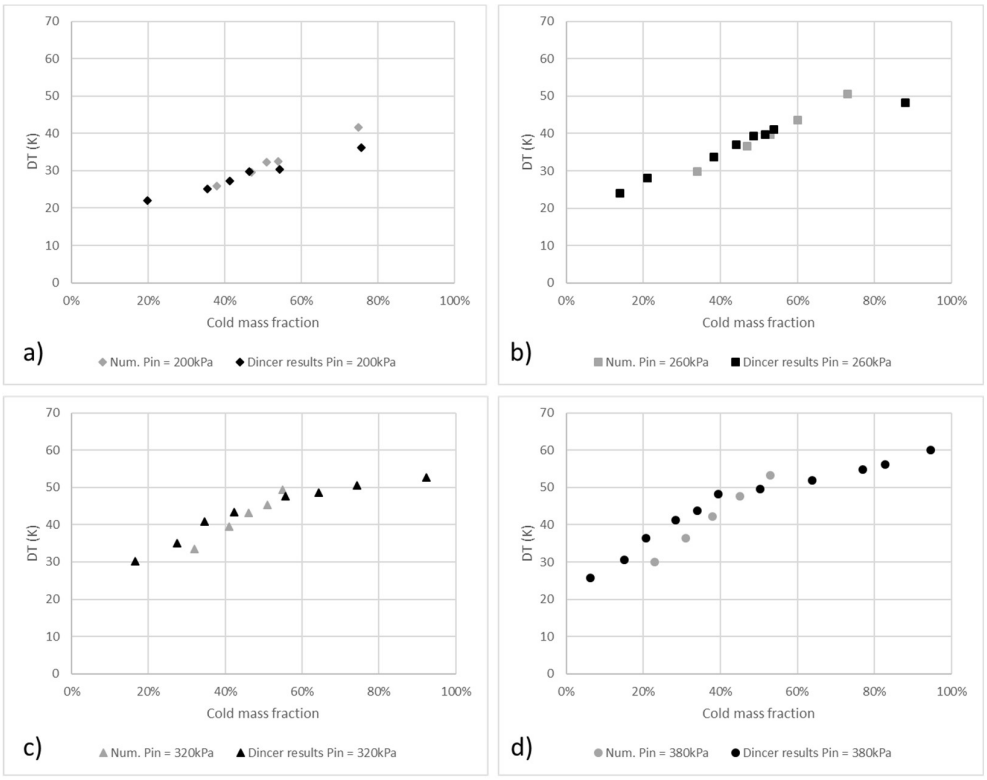

Fig. 5 Comparison of model results with experimental data (a : inlet pressure 200kPa, b : 260kPa, c : 320kPa, d : 380kPa)

Based on previous analysis, we decided to use the Realizable k-ε model in our study.

4. RESULTS AND DISCUSSION

In the following sections, the model developed is used to predict the impact of various parameters on the cold temperature gradient (ΔTc) of the vortex tube.

4.1 Impact of inlet pressure on performance

The impact of inlet pressure on cold temperature gradient has been assessed by varying it value between 2 bars and 15 bars while keeping cold outlet pressure at 0bars. Hot outlet pressure has been manually adjusted in order to reach a cold mass fraction of 50% and be able to compare the results.
As can be seen in Figure 6, there is a linear relation between total mass flowrate and inlet pressure. Regarding cold temperature gradient, it is positively correlated with inlet pressure between 2bars and

9bars. A maximum temperature gradient is observed when pressure reaches 10 bars (ΔTc = 94°C). When pressure is further increased, the cold temperature gradient does not increase any more.
This threshold in cold temperature gradient seems to be linked with the velocity of the cold stream. Indeed, a stagnation of average Mach number at the cold outlet is observed at high pressures, even though total mass flowrate still increases. This cold outlet velocity stagnation is simultaneous to cold temperature gradient stagnation, which suggests a possible link between the two phenomena.
To the authors' knowledge, this effect is not mentioned specifically in the literature. However, some experimental results (for example the ones presented by Kirmaci [23], Gao [15], Ambedkar and Dutta [24] or Cartlidge et al [25]) also exhibit a stagnation of cold temperature gradient at high cold mass fraction when inlet pressure increases.

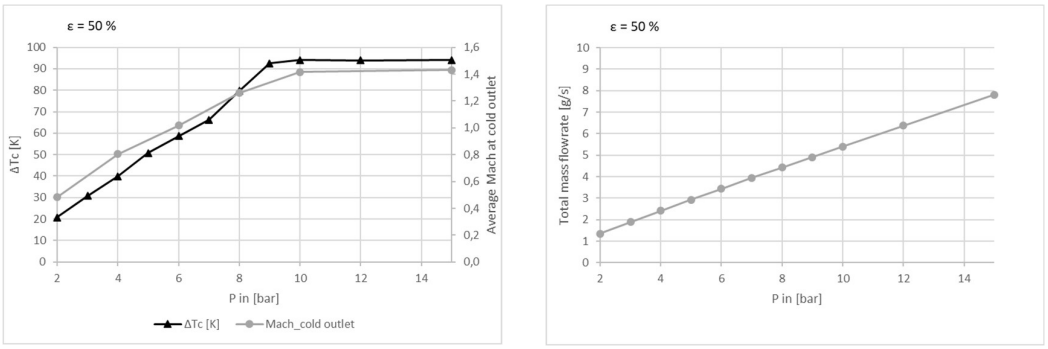

Fig. 6 Evolution of cold temperature gradient, average Mach number at cold outlet (left) and total mass flowrate (right) with inlet pressure (for cold mass fraction 50%)

4.2 Optimization of vortex tube design

Design Explorer module available in Ansys Fluent has been used in order to find the diameters for the tube and the cold inlet that maximize the cold temperature gradient. All other dimensions were kept constant. Two optimizations have been done, for four and six inlet nozzles. As previously, the hot outlet pressure has been manually adjusted in order to reach a cold mass fraction of 50% for all cases, so as to get comparable results.
Figure 7 shows the surface response obtained for the 6 inlet nozzles, using non-parametric regression.

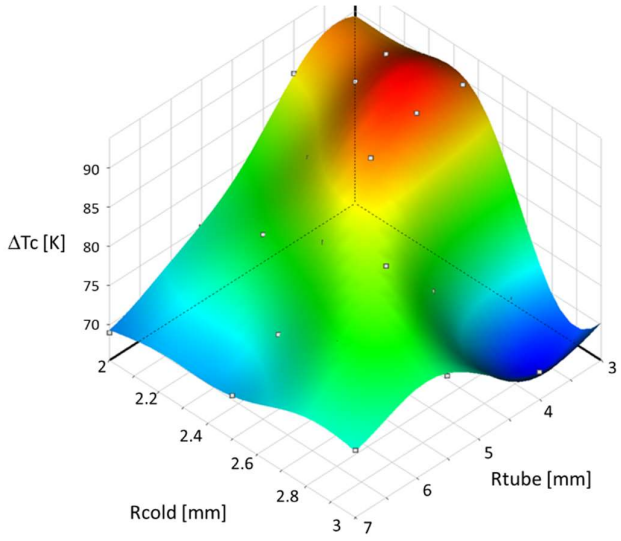

Fig 7 Surface response showing ΔTc as a function of Rtube and Rcold

The comparison of optimal to initial vortex tube dimensions is presented in Figure 8.

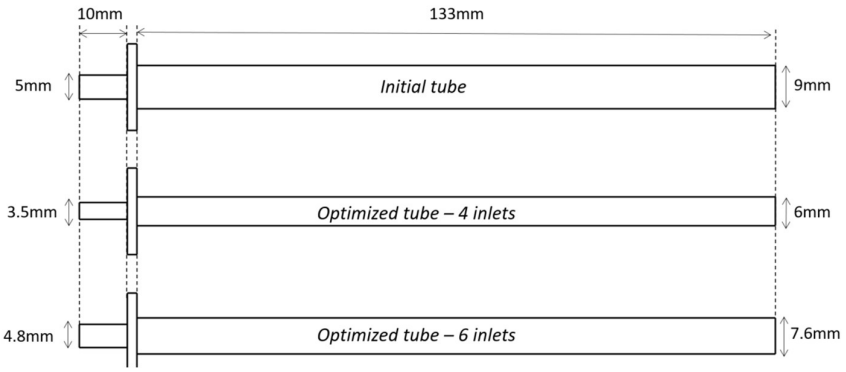

Fig. 8 Dimensions of optimized tubes compared to initial tube

The evolution of cold temperature gradient as a function of cold mass fraction is presented in Figure 9 for the three tube dimensions, and for two inlet pressures (2 bars and 6 bars). It is clear that both optimized tubes have a higher performance than the initial tube (cold temperature gradient increased by ~10 to 35°C), except at 6 bars inlet pressure and high cold mass fraction (over 75%). In addition, it can be seen that the optimized tubes with six inlet nozzles presents superior performance to the optimized tube with four nozzles over the whole range of cold mass fraction, and for the two inlet pressures.

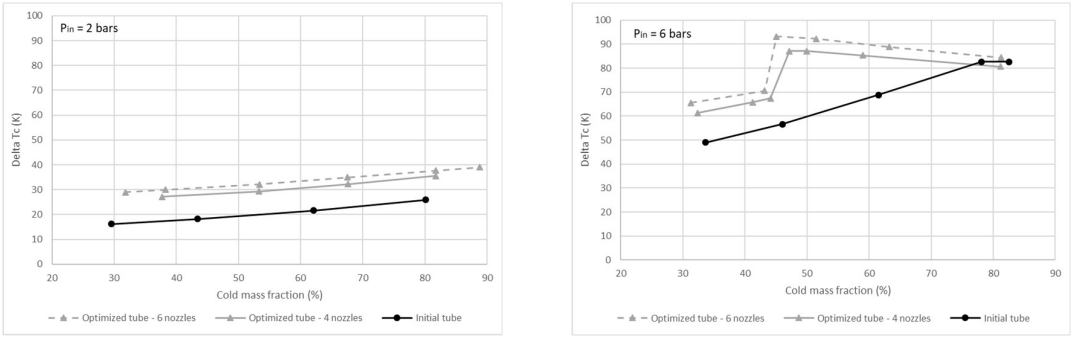

Fig. 9 Prediction of ΔTc as a function of cold mass fraction for initial and optimized tube. Left : Inlet pressure 2 bars, right : Inlet pressure 6 bars

A linear evolution of cold temperature gradient with cold mass fraction is observed for all tubes at 2 bars inlet pressure, which is consistent with some previous experimental and numerical results ([11], [18]). The evolution of cold temperature gradient with cold mass fraction with the initial tube at 6 bars inlet pressure is similar.

However, an unexpected behavior can be observed for the optimized tubes for 6 bars inlet pressure. At low cold mass fractions, cold temperature gradient increases gently with cold mass fraction. There is a sharp increase in ΔTc at a cold mass fraction ~45% (+20°C ΔTc achieved over a few percentage of cold mass fraction). After this critical step, a slight decrease in cold temperature gradient is observed when cold mass fraction increases further. In these cases, the evolution of cold temperature gradient with cold mass fraction is closer to the evolution observed by Markal et al [14] or Gao [15], that highlighted an optimum value of cold mass fraction. However, to the authors' knowledge, the sharp increase of cold temperature gradient over a small range of cold mass fraction has never been observed.

As can be seen in Figure 10, Mach number on the cold outlet presents high values at the center of the tube, and near the wall (with a value fixed at zero at the wall), and a minimum value at an intermediate radius (see Figure 10). However, differences can be observed between the profiles obtained just before and just after the critical cold mass fraction. Just before the critical cold mass fraction, maximum Mach number is observed at the center of the outlet. The flow is supersonic at the center and the periphery of the cold outlet, and subsonic in the intermediate region. Just after the critical cold mass fraction, the

flow is supersonic on the whole cold outlet (except near the wall), and maximum Mach number is located near lateral wall.
This observation suggests an association between vortex tube performance and flow velocity at the cold outlet, the achievement of high cold temperature gradient being linked to the occurrence of supersonic flow on the whole cold outlet.

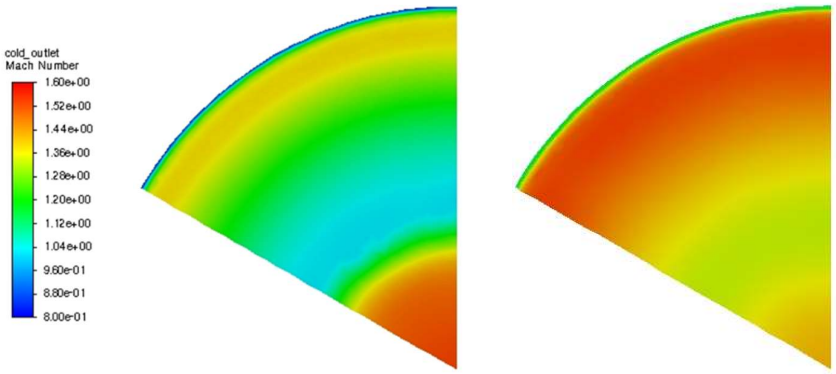

Fig 10 Visualization of Mach number on cold outlet at a cold mass fraction just below (left) and just over (right) the critical cold mass fraction

5. CONCLUSION

A 3D CFD model was created to investigate the energy separation mechanism within a cylindrical vortex tube. The model is based on the experimental study by Dincer et al. [19]. The simulation was developed in steady state using the Realizable k-ε turbulence model. There is a satisfactory agreement between the CFD results and the measured experimental data.
A geometric optimisation of tube diameters was conducted in order to maximize the cold temperature gradient of the device. Both optimized tubes outperform the initial tube, with a cold temperature gradient generally increased by ~10 to 35°C.
Two phenomena not mentioned specifically in the literature were observed in our simulations.
First, our study highlights the occurrence of a critical pressure, above which cold temperature gradient does not increase further even if inlet pressure increases. This effect is simultaneous to a stagnation in cold outlet velocity, which suggests a possible link between the two phenomena.
Second, a critical cold mass fraction was observed for the operation of vortex tubes at high pressure, at which cold temperature gradient increases by ~20°C. It appears that part of the flow at the cold outlet is subsonic below the critical cold mass fraction, while it is supersonic on the whole cold outlet above this value. This observation suggests an association between vortex tube performance and flow velocity at the cold outlet, the achievement of high cold temperature gradient being linked to the occurrence of supersonic flow on the whole cold outlet.
Further studies are recommended to further explore the subject. On the one hand, it would be interesting to reproduce experimentally the evolution of cold temperature gradient near critical cold mass fraction in order to evidence the jump in performance. On the other hand, specific numerical studies focussing on flow characteristics and Mach number distribution at the cold outlet could support the present observations and refine the understanding of the working process within a vortex tube.

REFERENCES

[1] G. J. Ranque, ‘Method and apparatus for obtaining from alpha fluid under pressure two currents of fluids at different temperatures’, 1,952,281, Mar. 27, 1934

[2] C. U. Linderstrøm-Lang, 'Gas separation in the Ranque-Hilsch vortex tube', *International Journal of Heat and Mass Transfer*, vol. 7, no. 11, pp. 1195–1206, Nov. 1964, doi: 10.1016/0017-9310(64)90061-4.
[3] Hilsch, Rudolf, 'The use of the expansion of gases in a centrifugal field as cooling process', *Review of Scientific Instruments*, vol. 18, no. 2, pp. 108–113, 1947.
[4] H. Takahama, H. Kawamura, S. Kato, and H. Yokosawa, 'Performance characteristics of energy separation in a steam-operated vortex tube', *International Journal of Engineering Science*, vol. 17, pp. 735–744, 1979.
[5] H. Takahama, 'Studies on vortex tubes', *Bulletin JSME*, vol. 8, pp. 433–440, 1965.
[6] V. Kirmaci and H. Kaya, 'Effects of working fluid, nozzle number, nozzle material and connection type on thermal performance of a Ranque–Hilsch vortex tube: A review', *International Journal of Refrigeration*, vol. 91, pp. 254–266, Jul. 2018, doi: 10.1016/j.ijrefrig.2018.05.005.
[7] Z. Hu, R. Li, X. Yang, M. Yang, R. Day, and H. Wu, 'Energy separation for Ranque-Hilsch vortex tube: A short review', *Thermal Science and Engineering Progress*, vol. 19, p. 100559, Oct. 2020, doi: 10.1016/j.tsep.2020.100559.
[8] H. R. Thakare, A. Monde, and A. D. Parekh, 'Experimental, computational and optimization studies of temperature separation and flow physics of vortex tube: A review', *Renewable and Sustainable Energy Reviews*, vol. 52, pp. 1043–1071, Dec. 2015, doi: 10.1016/j.rser.2015.07.198.
[9] S. Subudhi and M. Sen, 'Review of Ranque–Hilsch vortex tube experiments using air', *Renewable and Sustainable Energy Reviews*, vol. 52, pp. 172–178, Dec. 2015, doi: 10.1016/j.rser.2015.07.103.
[10] M. Yilmaz, M. Kaya, S. Karagoz, and S. Erdogan, 'A review on design criteria for vortex tubes', *Heat Mass Transfer*, vol. 45, pp. 613–632, 2009.
[11] X. Liu and Z. Liu, 'Investigation of the energy separation effect and flow mechanism inside a vortex tube', *Applied Thermal Engineering*, vol. 67, no. 1, pp. 494–506, Jun. 2014, doi: 10.1016/j.applthermaleng.2014.03.071.
[12] T. Dutta, K. P. Sinhamahapatra, and S. S. Bandyopadhyay, 'Experimental and numerical investigation of energy separation in counterflow and uniflow vortex tubes', *International Journal of Refrigeration*, vol. 123, pp. 9–22, Mar. 2021, doi: 10.1016/j.ijrefrig.2020.11.013.
[13] B. A. Shannak, 'Temperature separation and friction losses in vortex tube', *Heat and Mass Transfer*, vol. 40, pp. 779–785, 2004.
[14] B. Markal, O. Aydın, and M. Avcı, 'An experimental study on the effect of the valve angle of counter-flow Ranque–Hilsch vortex tubes on thermal energy separation', *Experimental Thermal and Fluid Science*, vol. 34, no. 7, pp. 966–971, Oct. 2010, doi: 10.1016/j.expthermflusci.2010.02.013.
[15] C. Gao, 'Experimental study on the Ranque-Hilsch vortex tube', Technische Universiteit, Eindhoven, 2005. [Online]. Available: 10.6100/IR598057
[16] N. Pourmahmoud, A. Hassan Zadeh, O. Moutaby, and A. Bramo, 'Computational Fluid Dynamics analysis of helical nozzles effects on the energy separation in a vortex tube', *Thermal Science*, vol. 16, no. 1, pp. 151–166, 2012.
[17] G. Agarwal, Z. P. McConkey, and J. Hassard, 'Optimisation of vortex tubes and the potential for use in atmospheric separation', *Journal of Physics D: Applied Physics*, vol. 54, p. 015502, 2021.
[18] U. Behera *et al.*, 'CFD analysis and experimental investigations towards optimizing the parameters of Ranque–Hilsch vortex tube', *International Journal of Heat and Mass Transfer*, vol. 48, no. 10, pp. 1961–1973, May 2005, doi: 10.1016/j.ijheatmasstransfer.2004.12.046.
[19] K. Dincer, S. Baskaya, B. Z. Uysal, and I. Ucgul, 'Experimental investigation of the performance of a Ranque–Hilsch vortex tube with regard to a plug located at the hot outlet', *International Journal of Refrigeration*, vol. 32, no. 1, pp. 87–94, Jan. 2009, doi: 10.1016/j.ijrefrig.2008.06.002.
[20] M. Baghdad, A. Ouadha, O. Imine, and Y. Addad, 'Numerical study of energy separation in a vortex tube with different RANS models', *International Journal of Thermal Sciences*, vol. 50, no. 12, pp. 2377–2385, Dec. 2011, doi: 10.1016/j.ijthermalsci.2011.07.011.
[21] A. Ouadha, M. Baghdad, and Y. Addad, 'Effects of variable thermophysical properties on flow and energy separation in a vortex tube', *International Journal of Refrigeration*, vol. 36, no. 8, pp. 2426–2437, Dec. 2013, doi: 10.1016/j.ijrefrig.2013.07.018.

[22] A. M. Alsaghir, M. O. Hamdan, and M. F. Orhan, 'Evaluating velocity and temperature fields for Ranque–Hilsch vortex tube using numerical simulation', *International Journal of Thermofluids*, vol. 10, p. 100074, May 2021, doi: 10.1016/j.ijft.2021.100074.
[23] V. Kırmacı, 'Exergy analysis and performance of a counter flow Ranque–Hilsch vortex tube having various nozzle numbers at different inlet pressures of oxygen and air', *International Journal of Refrigeration*, vol. 32, no. 7, pp. 1626–1633, Nov. 2009, doi: 10.1016/j.ijrefrig.2009.04.007.
[24] P. Ambedkar and T. Dutta, 'CFD simulation and thermodynamic analysis of energy separation in vortex tube using different inert gases at different inlet pressures and cold mass fractions', *Energy*, vol. 263, p. 125797, Jan. 2023, doi: 10.1016/j.energy.2022.125797.
[25] J. Cartlidge, N. Chowdhury, and T. Povey, 'Performance characteristics of a divergent vortex tube', *International Journal of Heat and Mass Transfer*, vol. 186, p. 122497, May 2022, doi: 10.1016/j.ijheatmasstransfer.2021.122497.